Supplementary Information for:

Concerning the selection of crystallization modifiers for non- hydrogen bonded systems: the case of benzophenone.

Adrian Hutchinson, Simon Black and Roger Davey

Department of Chemical Engineering and Analytical Science,

School of Engineering, University of Manchester, M13PL, UK

Contents

S1: Justification for cut-off at 4.70Å

S2: Comparison of N_{FC} and Interaction Energies

S3: Aromatic analyser results for BPHENO12

S4: Weaker Interactions in BPHENO11 and BPHENO12

S5: Solubility

S6: Crystallization/ Morphology screen

S7: Characterising doped crystals

S8: Measurement of Growth rates

S9: Additive Crystal Structures

S10: Strong and weak approaches in the crystal structures of additives

S11. Strongest Approaches in Benzene (BENZEN) and Graphite (YPOTUU02)

S1: Justification for Cut-off 4.70Å

UNI (see paper, reference 24) was selected to study the relationship between N_{FC} and energy in BZP. The lattice energy of BPHENO12 according to UNI is -105.5 kJ/mol. This is in good agreement with the value of -102.5kJ/mol calculated using HABIT in reference 14 of the paper. UNI is available within the Mercury software, facilitating comparison of UNI calculations to N_{FC}. The relevant formulae and parameters are given in tabular format in Table 1 in reference 24 of the paper and were used to plot the relationships between interatomic separation and energy for carbon and hydrogen atoms in Figure S1:

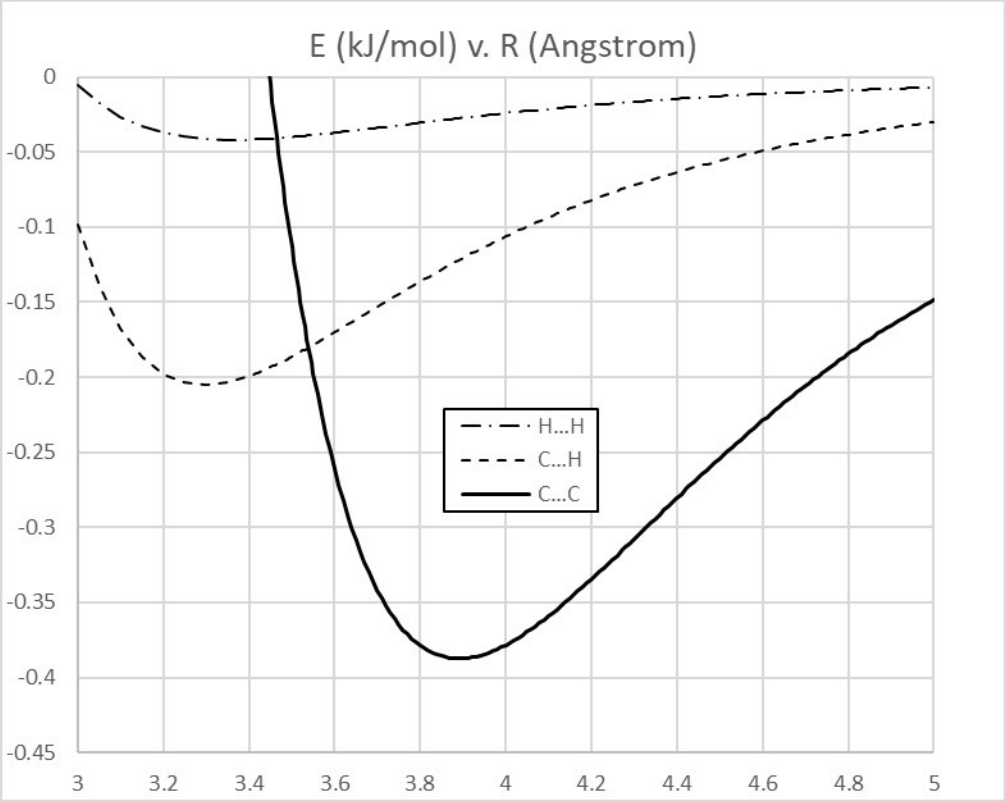

Figure S1.1: C…C, C…H and H…H energy as a function of interatomic separation.

The sum of the Van der Walls radii for C…C connections is 3.40Å. As can be seen from the plot, and Table 1 in reference 24 of the paper, the energy minimum for C…C connections is at 3.89Å. C…C connections out to 4.7Å are more attractive than all C-H and H-H connections.

Figure 1 also clarifies the rationale for the choice of 4.7Å as the cutoff. This excludes atom…atom connections with energies less than -0.21 kJ/mol. For each BZP…BZP interaction, this excludes all 260 C…H and 100 H…H connections. The remaining favourable connections, typically between 50 and 10, can be visualized together. Choosing a smaller cutoff value risks losing readily accessible information for no obvious benefit.

S2: Comparison of N_{FC} and Interaction Energies

Figure S2 compares N_{FC} with UNI Interaction energies for the ten BZP…BZP interactions described in the paper and the SI. The four strongest molecule-molecule pairings based on this geometric approach are also the four energetically most stable, as calculated by UNI. The correlation is also good for weaker BZP…BZP interactions.

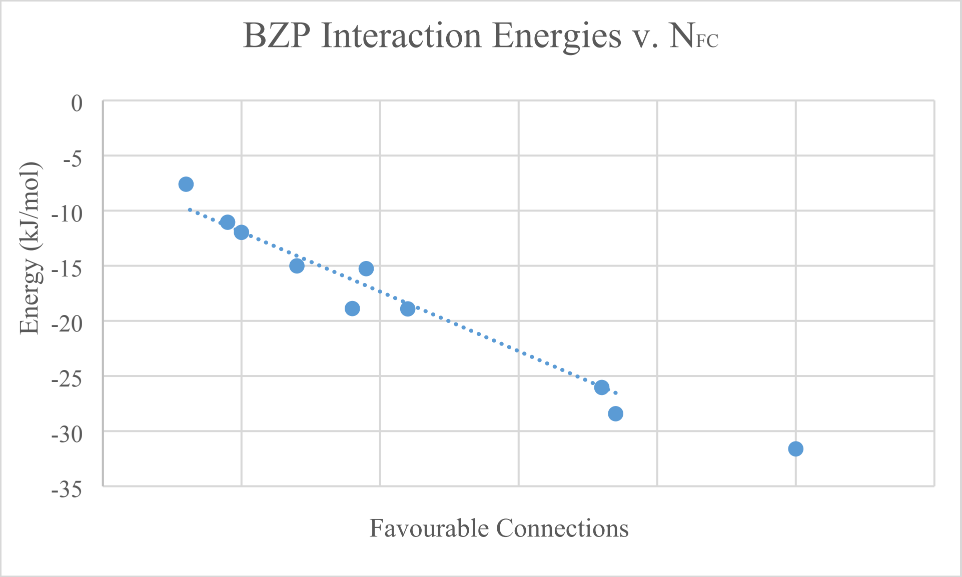

Figure S2.1: N_{FC} and Interaction Energies

Table S1 compares N_{FC} and UNI energies for the strongest interactions in the additive crystal structures:

Table S2.1: Favourable Connections and UNI Interaction Energies for Additives

Interaction	CSD reference	N_{FC}	E (kJ/mol)
4MBZP1	FEVNAV01	30	-26.1
4ABZP1	VOFVAN21	33	-28.8
4FBZP1	BOJVIH	43	-31.2
4MBZP2	FEVNAV02	47	-39.5
4ABZP2	VOFVAN23	81	-45.2
4NBZP1	BOJVON	88	-53.2

The geometric N_{FC} method ranks the interactions in the same order as the UNI calculations.

S3: Aromatic analyser results for BPHENO12

The aromatic analyser identifies six strong phenyl…phenyl approaches, in symmetry-related pairs, as shown in Table S1:

Table S3.1 "Strong" Approaches from the Aromatic Analyser Output for BPHENO12

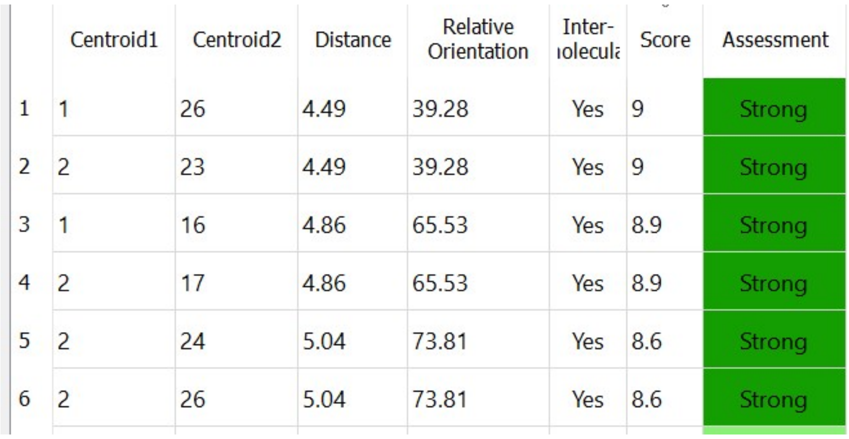

	Centroid1	Centroid2	Distance	Relative Orientation	Inter-ıolecula	Score	Assessment
1	1	26	4.49	39.28	Yes	9	Strong
2	2	23	4.49	39.28	Yes	9	Strong
3	1	16	4.86	65.53	Yes	8.9	Strong
4	2	17	4.86	65.53	Yes	8.9	Strong
5	2	24	5.04	73.81	Yes	8.6	Strong
6	2	26	5.04	73.81	Yes	8.6	Strong

Interaction BZP(1), as shown Figure 2 of the main manuscript, includes both the first phenyl…phenyl approach in the table ("skew", 18 favourable connections) and the fifth approach ("edge…face", 10 favourable connections). The second and sixth phenyl…phenyl approaches in the table are related by symmetry to the first and fifth interactions respectively.

Figure S3.1 was generated from the Aromatic Analyser output by manually deleting all but three molecules, and recolouring and relabelling the six remaining centroids (A = 1, A' = 2, B = 23, B' = 24, D' = 26). This clarifies which approaches in the table are part of the same intermolecular interaction. The figure also shows how the two molecules above and below the central molecule are related by translational symmetry along the *x* axis.

The third (and symmetry-related fourth) phenyl…phenyl approach in this table is discussed in more detail in section S4.2 below.

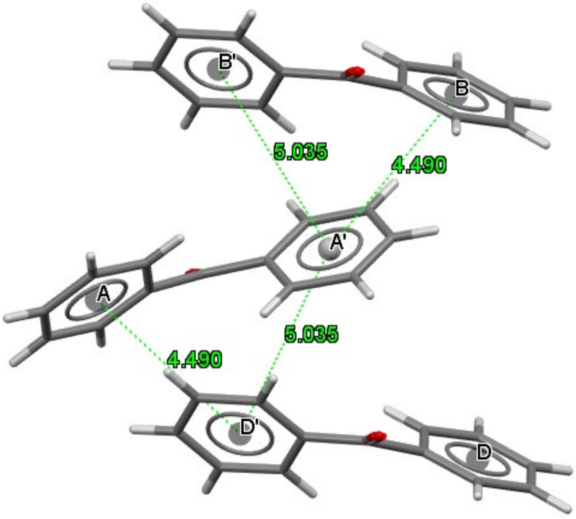

Figure S3.1 The Symmetry-related strongest intermolecular interactions in BPHENO12. The x axis is in the vertical direction.

S4 Weaker Interactions in BPHENO11 and BPHENO12.

The two strongest BZP…BZP interactions in BPHENO11 and BPHENO12 are described in the main text. Selected weaker interactions in these two structures are summarised in Table S4.1 and Figures S4.1 – S4.7.

Table S4.1: Weaker intermolecular interactions in BPHENO11 and BPHENO12.

Interaction	N_{FC}	Symmetry	Phenyl…phenyl approaches	Carbonyl approaches
BZP(3)	36	*y* screw axis	skew (17) + weak (7) + weak (5)	(7)
BZP(4)	22	*y* screw axis	edge…face (12)	(5 + 5)
BZP(5)	19	*y* screw axis	weak (9) + weak (4)	(6)
BZP(6)	18	2-fold rotation	weak (8) + weak (5) + weak (5)	-
BZP(7)	14	*z* screw axis	weak (7) + weak (3)	(4)
BZP(8)	10	inversion	weak (1)	(4 + 5)
BZP(9)	9	inversion	weak (1)	(4 + 4)
BZP(10)	6	*z* screw axis	weak (2)	(4)

BPHENO12 contains BZP(1), BZP(4), BZP(5), BZP(7), BZP(10)

BPHENO11 contains BZP(2), BZP(3), BZP(6), BZP(8), BZP(9)

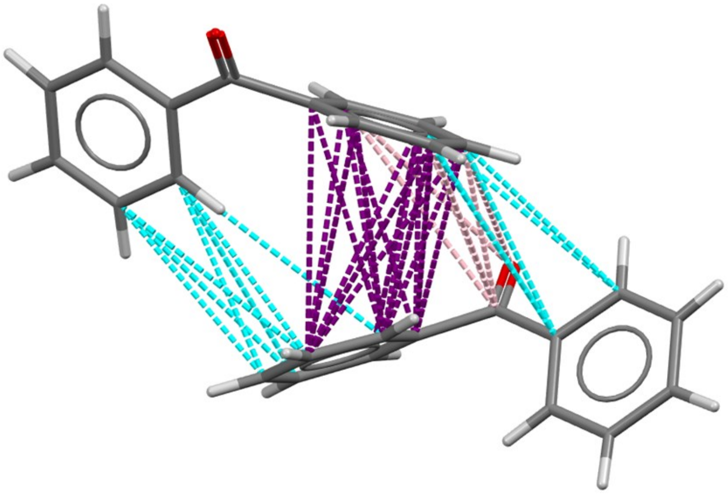

Figure S4.1 BZP(3), from BPHENO11. The y axis is in the vertical direction.

The BZP(3) interaction, Figure S4.1, is from the metastable polymorph BPHENO11. It is dominated by a “skew” approach, featuring the 17 favourable connections shown in purple. The approach links phenyl rings A1 and B1 (labels not shown), forming the 2-fold screw axis along the short b axis (8.12Å).This is supported by 7 favourable connections involving the neighbouring carbonyl group, shown in pink. The other 12 favourable connections, shown in cyan, are split between two weaker phenyl-phenyl interactions.

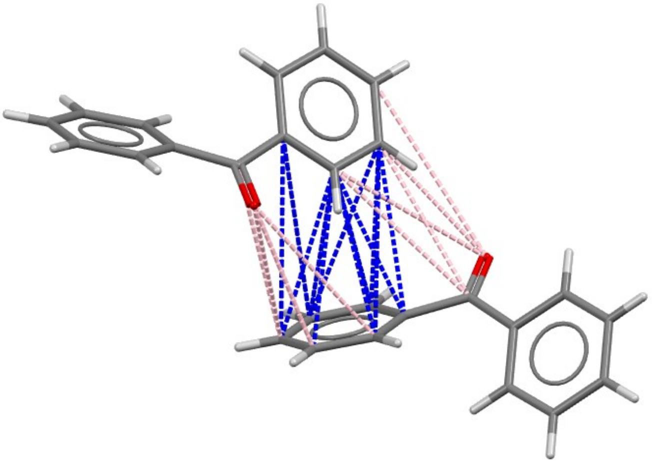

Figure S4.2 BZP (4), from BPHENO12. The *y* axis is in the horizontal direction.

BZP(4), Figure S4.2, is from the stable polymorph BPHENO12. The “edge…face” approach (N_{FC} = 12, shown in blue) is the other approach identified as “strong” by the aromatic analyser in Table S3.1 above. This is supported by two carbonyl…phenyl approaches (N_{FC} = 5 + 5, shown in pink). This interaction embodies the 2-fold screw axis in the *y* direction, fixing *b* =

10.24Å. These interactions link the molecules shown in Figure 8 of the main text. 4MBZP and 4ABZP molecules can replace one of the BZP molecules in this interaction without penalty. This accounts for the attachment of these additives on {011} surfaces.

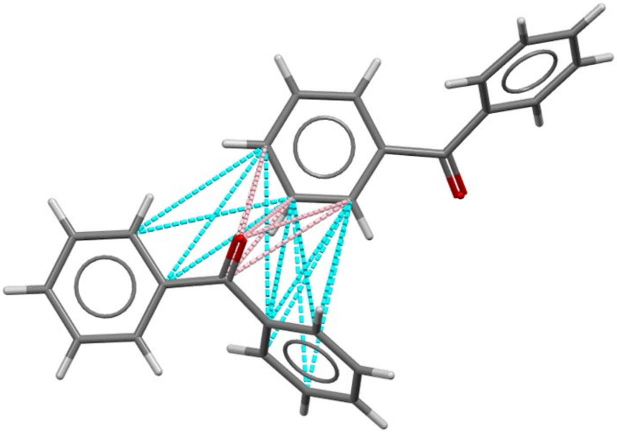

Figure S4.3 BZP (5), from BPHENO12. The *y* axis is in the horizontal direction.

Interaction BZP (5), Figure S4.3, is from the stable polymorph BPHENO12. It also embodies the 2-fold screw axis in the *y* direction, reinforcing BZP (4). The comments above concerning how additives may bind using similar interactions to BZP(4) also apply to BZP(5).

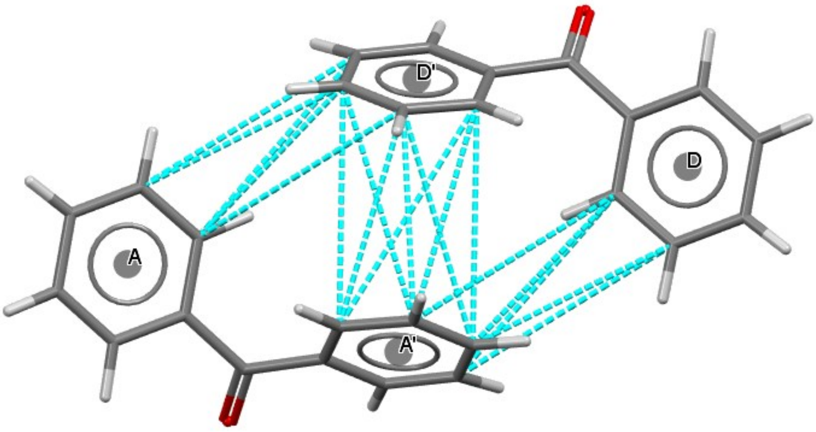

Figure S4.4: BZP (6), from BPHENO11, viewed along the two-fold rotation axis.

Interaction BZP(6), Figure S4.4, is form the metastable polymorph BPHENO11. It contains a central weak phenyl…phenyl aproaches (N_{FC} = 8) supportd by two weaker symmetry releated phenyl…phenyl approaches (N_{FC} = 5 each). The interaction embodies a 2-fold rotation axis.

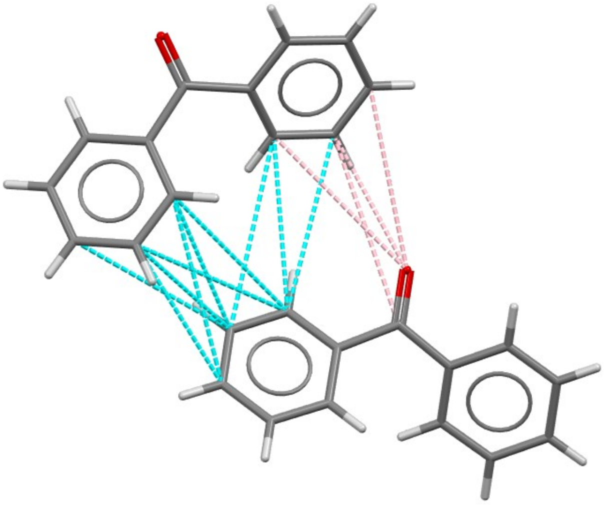

Figure S4.5: BZP(7), from BPHENO12

Interaction BZP(7), Figure S4.5, is from the stable polymorph BPHENO12. It contains a weak phenyl…phenyl aproach (N_{FC} = 7) and a weaker phenyl…phenyl approach supported by a carbonyl…phenyl approach (N_{FC} = 3 + 4) including the C…O connection at 3.43Å .

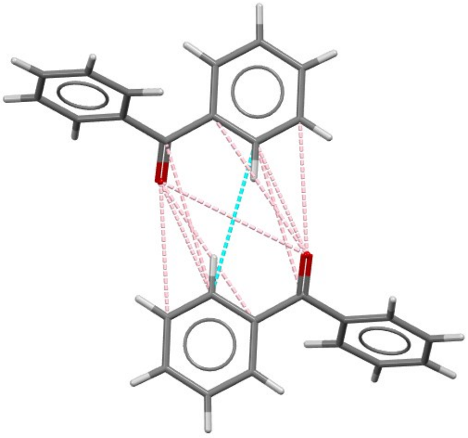

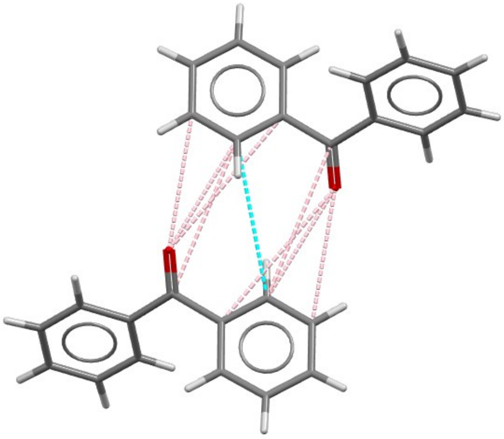

Figure S4.6: BZP(8) on the left and BZP(9) on the right, both from BPHENO11.

The two interactions, BZP(8) and BZP(9), (Figure 4.6) from the metastable form BPHENO11 are both centrosymmetric and dominated by carbonyl…phenyl interactions, which include C…O interactions of 3.41Å (left) and 3.45Å (right).

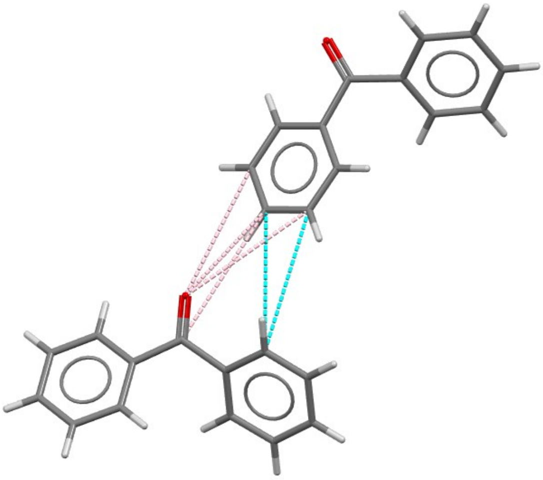

Figure S4.7: BZP(10), from BPHENO12

BZP(10), Figure S4.7, is the interaction from BPHENO12 which appears on the left in Figure 8 of the main text. $N_{FC} = 6$, four of which are carbonyl…phenyl connections, including the C…O connection at 3.45Å.

S5: Solubility

The solubility of BZP was determined gravimetrically at 15°C both in pure IPA and in the presence of the additives. Slurries of excess BZP in propan-2-ol were prepared and stirred at a constant temperature of 15°C using a jacketed vessel (sealed with a ground glass stopper) and connected to a Haake water bath. The solutions were allowed to equilibrate for 72 hours in pure solubility measurements and 24 hours for solubility measurements in the presence of additive. After equilibration the magnetic stirring was stopped and the solution was allowed to settle before a sample (approx. 1.5mL) was removed using a syringe and transferred (via a syringe filter) to a pre-weighed oven dried glass vial. The vial was re-weighed with the solution and left for the solvent to evaporate. Once all solvent had evaporated (confirmed by no further weight loss of the sample over a 24 hour period) the weight of the vial is recorded. For solubility measurements in the presence of additives, amounts of varying mole fraction of additive were added with respect to the solute. The additive was added to the solvent and fully dissolved before solute was added to the solution. Solubility measurements in the presence of additives assume a uniform distribution of additive in the solvent, so that the amount of final solid can be corrected to give the solubility of BZP. In samples with additive added (never in pure solutions), after evaporation of the solvent from the sample, the solute product was frequently a liquid which appeared to be more viscous than the original solution. The liquid was quite stable and remained in this state for long periods of time unless agitated. In some cases there were small crystals on the side of the vial away from the solution and upon contact of a crystal with the liquid, crystallisation of the remaining liquid occurred. Agitation caused the solution to crystallise and in some cases severe shaking was required. This was not observed in pure samples after evaporation where the product was solid. Thus, the post evaporation product is thought to consist of a metastable undercooled melt (BZP m.p. 49°C). Overall, this phenomenon contributed to uncertainties in the gravimetric measurement of solubility.

The equilibrium solubility of BZP in pure propan-2-ol solutions was measured as 0.171 ± 0.0025g/g (solute/solvent) at 15˚C. The solubility of BZP increased with the addition of the chosen additive molecules (concentrations up to 0.1 mole fraction). The data are shown in Table S5.1.

Table S5.1: A summary of the change in solubility in the presence of additive molecules.

Additive (x = 0.1)	**Solubility g per g**
Pure	0.17
4ABZP	0.23
4MBZP	0.20
DPA	0.24
DPM	0.21
DPE	0.22
2MBZP	0.22
3ClBZP	0.23
4FBZP	0.19
4NBZP	Not Soluble

S6: Crystallization/ Morphology screen

Cooling crystallisation were performed in a 50ml jacketed vessel. A desired amount of BZP (chosen to give a specific supersaturation at 15°C) was weighed and added to the vessel along with 10g of solvent. The solution was heated to dissolve the excess solid and then cooled to 15°C to generate supersaturation. The supersaturation of a solution was defined as:

$$\sigma = \ln\left(\frac{x_{ss}}{x_{eq}}\right)$$

x_{ss} is the solution concentration in mole fraction and $x_{eq}$is the equilibrium solubility of solute expressed in mole fraction.

Seed crystals of BZP were used in crystal growth rate measurements and these were grown from pure propan-2-ol solutions using a slow cooling crystallisation. The seed crystals were isolated and dried using vacuum filtration. Seed crystals used in growth experiments were typically 100x100μm.

S7: Characterising doped crystals

S7.1: HPLC methodology.

High Performance Liquid Chromatography (HPLC) was used to analyse dissolved samples of BZP grown in the presence of additives. A Varian Star HPLC with an auto sampler and UV-detection at 254nm was used in this body of work. A 250 x 4.6 mm Phenomenex Hyperclone C8 BDS column with 5µm particle and 130Å pore sizes was used for all chromatography in conjunction with a mobile phase consisting of a 50:50 mixture of acetonitrile and water at a flow rate of 1mL/min. Two 20µL injections were performed for each sample tested. Samples of BZP were dissolved in propan-2-ol to desired concentrations (approx. 80-100µg/mL). Calibration curves of 4MBZP, 4ABZP and DPM were all measured to allow calculation of concentrations of additive in samples of BZP. The area of the peak in the chromatogram of a pure additive sample was plotted against the concentration. A stock solution of sample was created and diluted allowing a range of concentrations to be tested. The relationship between peak area and concentration allows the concentration of additive in the sample to be determined. Sample concentrations of 1-20µg/mL were used to construct the calibration curves for 4MBP and 4ABP and concentrations of 2-40µg/ml for DPM.). In an attempt to determine whether the additive molecule is bound only to the crystal surface or whether it is incorporated into the crystal, two samples were tested. Firstly a sample of the filtered product, secondly some of the filtered product was washed with cold solvent in an attempt to remove additive molecules bound to the surface. Hence, in the washed samples if additive was present in the chromatogram it can be assumed that the additive is incorporated into the lattice and not only bound to the surface. Standard elution times are given in Table S7.1.

Table S7.1: A summary table of elution times of BZP and the additive molecules.

Molecule	Approximate Elution Time (mins)
BZP	9
4MBZP	12
4ABZP	5
DPM	18

From these it is evident that the presence of additives in samples of BZP should be detected since the elution times for all four molecules are all significantly different.

S7.2 XRD. Figure S7.2 shows powder diffraction patterns of samples grown in the presence of additives. The samples were unground and it is clear that preferred orientation occurs in all three BZP samples. The {011} crystal planes of the predicted powder pattern of BZP are labelled matching the preferred orientation peaks, (011), (022) and (033). Thus, it is confirmed that the {011} surfaces are more prevalent in the doped samples and that the effects seen in bulk crystallisations are the same as seeded crystal growth experiments. The peaks corresponding to the (022) planes are slightly shifted, compared to the pure BZP pattern, whilst the (011) and (033) peaks match quite well.

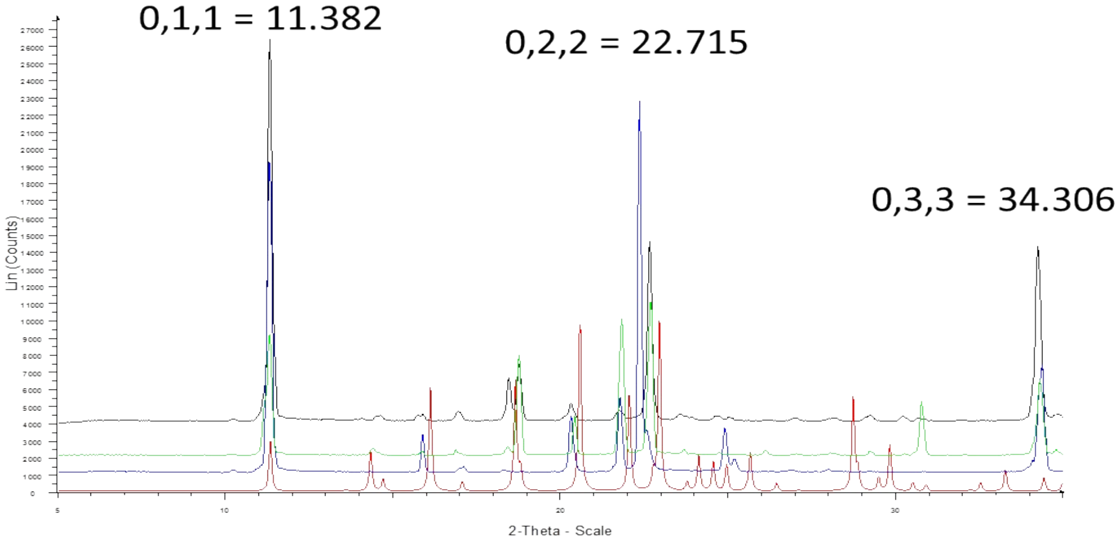

Figure S7.2 Powder X-ray diffraction patterns of benzophenone samples grown in the presence of additives. The calculated powder pattern of BZP is in red, the sample grown in the presence of 4ABZP is in black, the sample grown in the presence of 4MBZP is in blue and the sample grown in the presence of DPM is green.

S8: Measurement of Growth rates

A growth cell, 6 cm diameter and described elsewhere[1] was connected to a circulating water bath and placed under the objective of a Zeiss Axioplan 2 optical microscope. A solution of BZP and propan-2-ol (typically 5g) of desired supersaturation was added to a jacketed vessel and heated to dissolve any traces of solid. An amount of BZP solution (ca 3mL) was transferred to the growth cell along with a BZP seed crystal. The solution was then heated slightly to partially dissolve the seed crystal and completely dissolve any crystals which may have formed (during the agitation) during transportation of the solution. The temperature was then reduced to 15°C to generate supersaturation. Growth measurements were performed at 15°C to reduce the possibility of solvent evaporation. Photographs (under magnification of 25x) of the crystal were continuously taken every 30 seconds for a period of time (up to approximately 48 hours) or until the crystal had grown too large to measure. Figures S8.1 and S8.2 shows images of the crystal growing over time and the red lines on the individual images show the length and width measurements taken. The average growth rate of the crystal is calculated from these measurements of crystal dimensions over time; a different seed was used for each measurement. Experiments found to have more than one crystal in the cell were discarded since the calculated supersaturation is not accurate. Growth measurements in the presence of additives were performed in the same fashion, except the additive was added to the solution in the jacketed vessel. The amount of additive added to the solution was proportional to the benzophenone only. Hence a 10% additive concentration is calculated as 0.1 mole fraction of the total solid in solution.

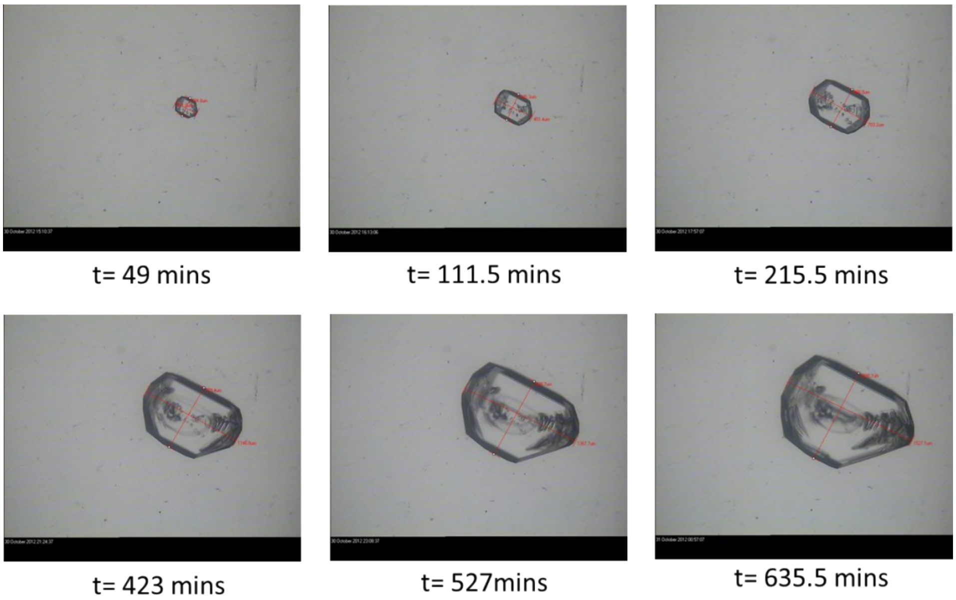
t= 49 mins

t= 111.5 mins

t= 215.5 mins

t= 423 mins

t= 527mins

t= 635.5 mins

Figure S8.1 Typical images of a growing crystal from which growth rates were determined.

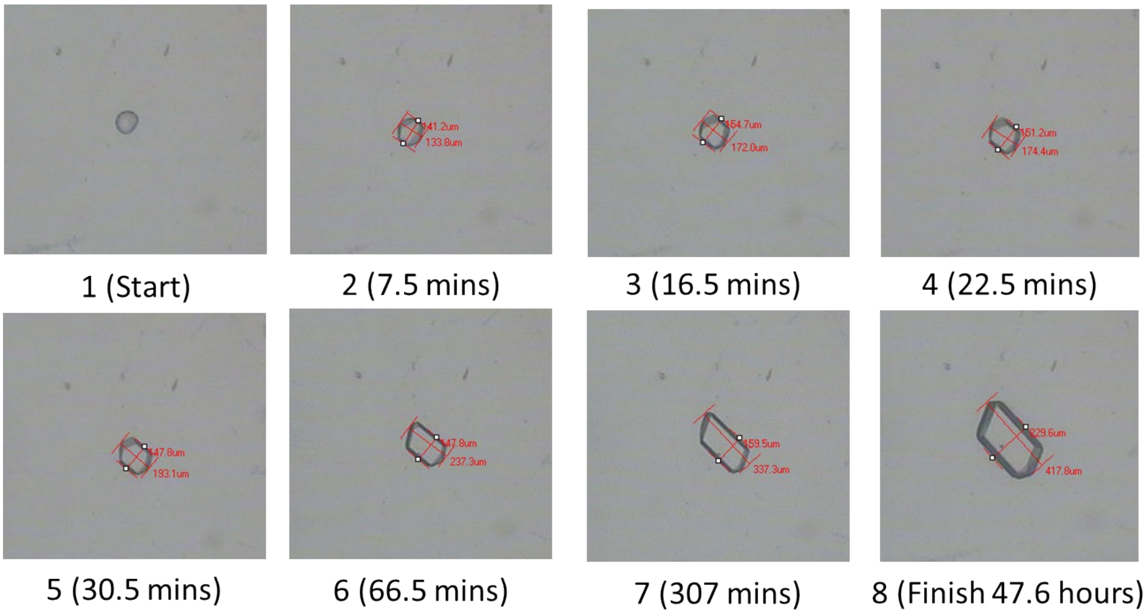

1 (Start)

2 (7.5 mins)

3 (16.5 mins)

4 (22.5 mins)

5 (30.5 mins)

6 (66.5 mins)

7 (307 mins)

8 (Finish 47.6 hours)

Figure S8.2 Typical images of a BZP crystal growing in the presence of 4MBZP (10%) at σ = 0.04.

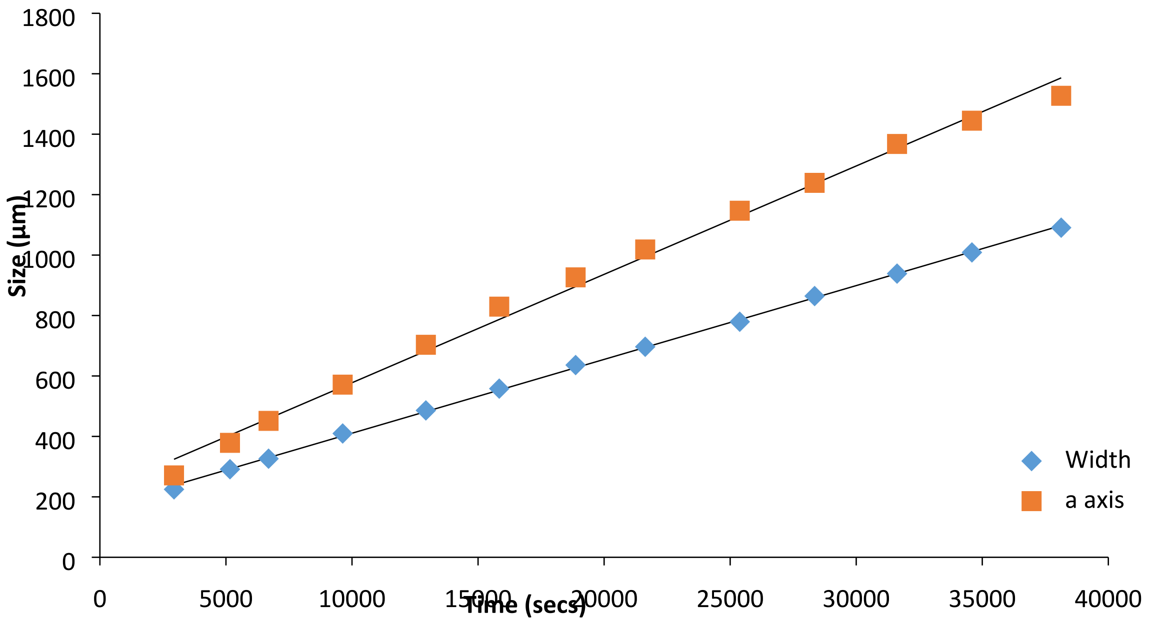

Figure S8.3 An example of the distance – time plot, the slope of which gives the growth rate.

S9: Additive Crystal Structures

Table S9.1: Additive Crystal Structures

Name	CSD Ref	Notes	Space Group	Strongest Interaction
BZP	BPHENO12	Stable	$P2_12_12_1$	BZP(1)
BZP	BPHENO11	From melt	C2/c	BZP(2)
4MBZP	FEVNAV01	stable	$P2_1/c$	4MBZP(1)
4MBZP	FEVNAV02	From melt	$P3_1$	4MBZP(2)
4ABZP	VOFVAN21	stable	$P2_1$	4ABZP(1)
4ABZP	VOFVAN23	P= 1.0GPa	$P2_1$	4ABZP(2)
4NBZP	BOJVON		$P2_1/n$	4NBZP(1)
4FBZP	BOJVIH	H/F disorder	$P2_1/n$	4FBZP(1)
DPA	QQQBVP02	Z’=8	P-1	n/a
DPM	ZZZMKS01	No hydrogens	$P2_1/c$	n/a

S10: Strong and weak approaches in the crystal structures of additives

Table S10.1: Approaches and Favourable Connections (N_{FC}) in Figure 7.

Fig.	Name	Strongest ph…ph	Next ph…ph	Other, weak ph…ph	Carbonyl	Substituents
7f	4MBZP (1)	Weak (7)	Weak (7)	(7)	(7)	Methyl (2)
7c	4ABZP (1)	Weak (8)	Weak (7)	(6)	(10)	Amine (2)
7e	4FBZP(1)	Edge…face (14)	Edge…face (13)	(2)	(12)	Fluorine (2)
7b	4MBZP (2)	Skew (21)	Weak (8)	(4) + (4)	(7)	Methyl (3)
7d	4ABZP (2)	Face…face (25)	Face…face (25)	(5)	(21)	Amine (5)
7a	4NBZP (1)	Face…face (26)	Face…face (25)	(3) + (1)	(16)	Nitro (17)

The colour scheme used for favourable connections in Figure 7 is consistent with Figures 2 and 3 in the main text and Figures S4.1 – S4.7 and S11.1 in this document:

Skew	purple
Edge…face	blue
Face…face	green
Weak	cyan
Carbonyl	pink
Substituents	orange

S11. Strongest Approaches in Benzene (BENZEN) and Graphite (YPOTUU02)

The strongest approach in BENZEN is the edge…face phenyl…phenyl approach shown in Figure S11.1. This approach is also rated “strong (8.6) “ by the aromatic analyser. The UNI energy is -8.4kJ/mol. Each molecule “donates” edge…face twice and “accepts” edge…face twice – occupying both faces. The molecules are related by 2-fold screw axes, fixing the *a* and *c* repeats at 7.44Å and 6.92Å respectively.

The strongest approach in graphite, while not strictly a phenyl-phenyl approach, is the archetypical approach for π – π stacking. The figure shows this approach of two 6-membered carbon rings in adjacent layers. The approach is centrosymmetric with 29 favourable connections, fixing the interplanar separation (c/2= 3.36Å) and offset.

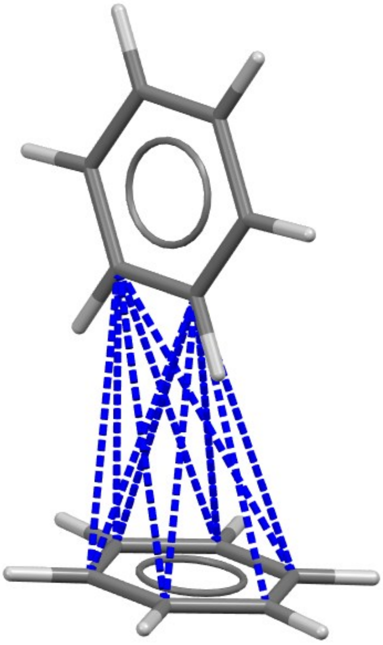

Figure S11.1: Strongest Approaches in BENZEN (left) and YOPTUU02 (right)

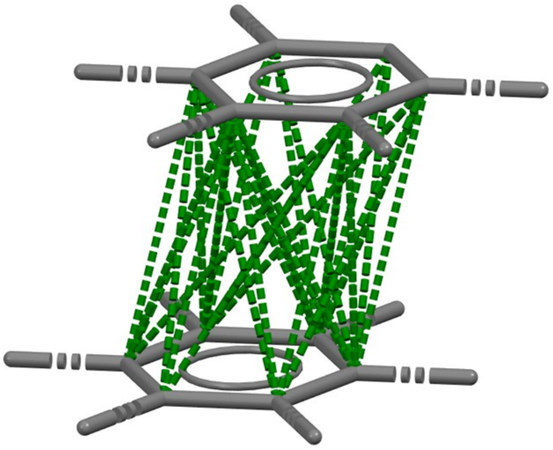

References.

1. R. Dowling, R. J. Davey, R. A. Curtis, G. Han, S. K. Poornachary, P. S. Chow and R. B. H. Tan, *Chem. Commun.* 2010, 46, 5924-5926.